SCIENTIFIC REPORTS

OPEN

SUBJECT AREAS:
TARGETED THERAPIES
SCIENTIFIC DATA

Received
14 February 2014

Accepted
19 May 2014

Published
10 June 2014

Correspondence and requests for materials should be addressed to E.R. (ruoslahti@sanfordburnham.org)

Quantity and accessibility for specific targeting of receptors in tumours

Sajid Hussain[1,2], Maria Rodriguez-Fernandez[3], Gary B. Braun[1,2], Francis J. Doyle, III.[3] & Erkki Ruoslahti[1,2]

[1]Cancer Research Center, Sanford-Burnham Medical Research Institute, La Jolla, California 92037, USA, [2]Center for Nanomedicine, and Department of Cell, Molecular and Developmental Biology, University of California Santa Barbara, Santa Barbara, CA 93106-9610, USA, [3]Department of Chemical Engineering, University of California Santa Barbara, Santa Barbara, CA 93106-5080, US.

Synaphic (ligand-directed) targeting of drugs is an important potential new approach to drug delivery, particularly in oncology. Considerable success with this approach has been achieved in the treatment of blood-borne cancers, but the advances with solid tumours have been modest. Here, we have studied the number and availability for ligand binding of the receptors for two targeting ligands. The results show that both paucity of total receptors and their poor availability are major bottlenecks in drug targeting. A tumour-penetrating peptide greatly increases the availability of receptors by promoting transport of the drug to the extravascular tumour tissue, but the number of available receptors still remains low, severely limiting the utility of the approach. Our results emphasize the importance of using drugs with high specific activity to avoid exceeding receptor capacity because any excess drug conjugate would lose the targeting advantage. The mathematical models we describe make it possible to focus on those aspects of the targeting mechanism that are most likely to have a substantial effect on the overall efficacy of the targeting.

Ligand-directed (synaphic) targeting is a therapeutic strategy that makes use of antibodies, peptides, small molecules, or other moieties that bind to molecular receptors specifically expressed in tumours[1]. Affinity to a target results in higher drug concentration at the diseased site than would be attained without targeting, increasing therapeutic efficacy and reducing toxicity to healthy tissues. Markers present on the vasculature of tumors are particularly favorable as targets because they are accessible to circulating probe, whereas receptors on tumor cells and other non-vascular cells are more difficult for a macromolecular drug to reach. Often under-appreciated in the field of targeted cancer therapy is that the efficiency for synaphic targeting is constrained by the quantity of accessible receptor – often a small and variable fraction of the total amount expressed in the tissue.

In this report we quantify accessibility of two commonly targeted tumor cell receptors, HER2 and αvβ3 integrin. We use computational modeling to examine the vascular and intratumoral delivery using experimental values for accessible and total receptor count. The computational model enables systems level analysis of the key components of the synaphic targeting process. Furthermore, it allows the comprehensive study of a variety of conditions that would be difficult to conduct experimentally. We further examine the effect of the recently discovered iRGD peptide[2], which when administered systemically increases the penetration of a co-administered drug into tumors[3].

Results

Biotinylation of accessible proteins in vivo. To assess the fraction of tumor proteins accessible to a blood-borne probe, we first determined the total amount of the two receptors we had chosen for this study: the first was the αv integrins, which are highly expressed in tumor vasculature, tumor cells and tumor fibroblasts[4] and much used in synaphic drug targeting[1,5]. The second receptor was the HER2 tyrosine kinase receptor, the gene which is frequently amplified in breast cancer and drives tumor development and progression[6,7]. HER2 is also commonly used as a target for drug delivery. ELISA quantification provided a baseline value on the amount of αv integrins and HER2 in tumors (Tables 1 and 2).

To determine the fraction of αv integrins accessible to a blood-borne probe, we perfused tumor-bearing mice with the amine reactive ester derivative of biotin (sulfo-NHS-LC-biotin)[8]. We obtained high degree of labeling of tumor vessels in 4T1 and M21 tumors (Figures 1 and S1), higher than what was seen in Rybak et al. (2005). A possible explanation is that we used orthotopic tumors, which are thought to have a better perfused vasculature than the subcutaneous xenograft tumors used by Rybak et al.[9]. In addition, we examined tumor periphery, which is relatively well vascularized.

Table 1 | Total tumor cell integrin αvβ3 and those accessible to *in vivo* biotinylation in 4T1 and M21 tumors, with (+) and without (−) iRGD pre-injection

Tumor	Integrin αvβ3	pmol/g tumor[$]	# receptors/cell * (×10³)	% accessible receptors
4T1	Total	170 ± 15	102 ± 8	-
	Biotin-labeled (−iRGD)	7.5 ± 0.7	4.4 ± 0.4	4.3
	Biotin-labeled (+iRGD)	33.3 ± 1.6	20 ± 1	20
M21	Total	340 ± 20 (h + m)	205 ± 3	-
	Biotin-labeled (−iRGD)	31 ± 3.6 (h) + 4.7 (m)	18.9 ± 2.1 (h) + 2.8 (m)	9
	Biotin-labeled (+iRGD)	130 ± 5 (h)	78 ± 3	38

The accessible and total receptors were measured by ELISA as described under ''Materials and Methods''. Data are presented as the mean ± SD (n = 3).
[$]**h** denotes human component; **m** denotes mouse component.
*Assuming 10^9 cells per gram of tumor tissue[10].

Quantification of the fraction of biotinylated αvβ3 integrin in the 4T1and M21 tumor models showed that in the 4T1 mouse breast tumor the fraction of biotin-accessible αvβ3 was ~4% of the total (7.5 ± 0.7 of a total of 170 ± 15 pmol/g; Table 1). Assuming that there are 10^9 cells in a gram of tumor[10,11] this translates to an accessible average of 4.4 ± 0.4 × 10^3 receptors per cell. The M21 (human melanoma) model had higher biotin probe accessibility than the 4T1 model, with 9% of the total human αvβ3 being labeled in M21 (Table 1), 31 ± 3.6 of a total 340 pmol/g. This value should be noted as an underestimate since it does not include the mouse αvβ3 contributed by the non-tumor cells in the tumors (Table S4). In BT474, a human breast cancer model, the quantity of HER2 reactive with the biotinylation compound was found to be approximately 10-fold greater than that of αvβ3 integrin in the other models, with 105 ± 13 of a total 1850 ± 150 pmol HER2 per gram, corresponding to an accessible quantity of 6.3 ± 0.8 × 10^4 molecules/cell (Table 2). Notably, despite the greater total quantity of labeled HER2 compared to αvβ3 integrin in the other models, the accessibility of HER2 was similar at 5.7% of total receptor.

Effect of iRGD on receptor biotinylation. The tumor-penetrating peptide, iRGD (sequence: CRGDK/RGPDC), is capable of enhancing the delivery of co-administered drugs to tumours[3]. We next tested whether iRGD would increase accessibility of αvβ3 and HER2 to the circulating biotinylation probe. The iRGD effect is transient; it peaks at 30 min and is essentially over at 1 hour, presumably because the half-life of the peptide in the circulation is short, about 10 min. We limited our analysis to one administration of the peptide to emphasize that we are measuring accessibility and that it can be modulated. Repeated administration of iRGD has been used previously and does enhance long-term antibody accumulation in tumors[3]. iRGD was intravenously injected into mice bearing 4T1 or BT474 tumors, followed 30 min later by perfusion with the biotinylation reagent and comparison to control-injected tumor mice. Tissue biotin distribution was visualized in tumor sections using streptavidin-Alexa Fluor 488 (Figure S1a). The results revealed 4 to 6-fold increased biotinylation of tumor αvβ3 and HER2 when iRGD was pre-injected (Tables 1 and 2).

Effect of iRGD on antibody accumulation in tumors. Pre-injection of iRGD into mice bearing 4T1 tumors (αv integrin antibodies) or BT474 tumors (anti-HER2 trastuzumab) 30 min prior to the antibody greatly increased antibody accumulation in the tumors as detected by fluorescent microscopy (Figure 2a). Quantification of the antibodies in tumor homogenates by ELISA showed that iRGD increased the tumor accumulation of both antibodies by 4 to 5-fold (from 16.6 to 77.4 pmol/g in 4T1 and from 27.1 to 128 pmol/g in BT474) (Table 3). Converted to percentage of accessible receptors, it increased from 10% to 43% in the 4T1 model and from 1.5% to 6.8% in the BT474 model.

In silico modeling and parameter estimation. We used computational modeling to examine and interpret the implications of the experimental results described above. Our mathematical model describes the uptake and retention of a circulating probe in vascularized tumors and captures the major processes that determine the time course of the probe concentration within a tumor including local and systemic clearance, extravasation, diffusion, binding, release, endocytosis, recycling, and degradation (**see Materials and Methods section for details**). The model considers that a circulating probe passes first through the vessel wall, with a dependence on its molecular weight, and then diffuses through the non-vascular tumor tissue (Figure 3). We used our experimental antibody results for quantities of total receptor, obtained other specific constants from literature, and estimated the rest of the parameters from the injected antibody experiments using parameter estimation techniques (Supporting Information and Table S1). Considering the % ID/g as the primary observable for injected antibody experiments, we fitted the model to antibody found in the tumor tissue after an injection of anti-mouse αv (4T1 tumor mice) or trastuzumab (BT474 tumor mice) each at 1 h circulation, to match with ELISA experiments.

The tissue vascular permeability, P, and the diffusion coefficient of the non-vascular tumor tissue, D, were assumed to be equal for 4T1 and BT474 tumor types when iRGD was not present, and literature values were used (P = 3e-9 m/s, D = 1e-11 m^2/s; Table S2). To consider the iRGD experiments, we performed a sensitivity analysis to determine how %ID/g at 1 h changes when each of the parameters is varied by the same small percentage (Supporting Information, Figure S2). This analysis revealed that changes in P have a much greater impact on the antibody uptake than changes in any other parameter that could be affected by iRGD (e.g., D, antibody affinity, endocytosis rate, clearance rate, and half-life of the antibody); therefore, we concluded that iRGD has a significant effect on the

Table 2 | Total and *in vivo* biotin accessible HER2 receptor in BT474 tumors, with (+) and without (−) iRGD pre-injection

HER2	pmol/g tumor	# receptors/cell (×10⁴)	% accessible receptors
Total	1850 ± 150	111.4 ± 9.1	-
Biotin-labeled(−iRGD)	105 ± 13	6.3 ± 0.8	5.7
Biotin-labeled (+iRGD)	613 ± 85	36.8 ± 4.8	33.1

The accessible and total receptors were measured by ELISA as described under ''Materials and Methods''. Data are presented as the mean ± SD (n = 3).

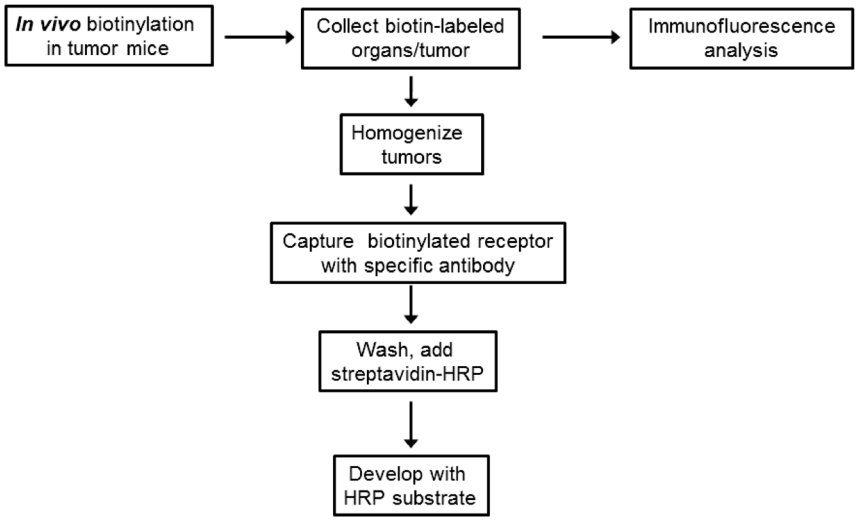

Figure 1 | **Schematic representation of the analysis of accessible receptors in tumor bearing mice by using the *in vivo* biotinylation method.**

permeability, and estimated the change in P for the iRGD experiments. We also estimated the radius of the Krogh cylinder (R_{Krogh}), the amount of tissue supplied by a capillary, since the degree of vascularization can vary between tumor types (Figure 3). In the fitting of P and R_{krogh} we included data corresponding to the %ID of antibody per gram tumor from both conditions with iRGD and without iRGD and assumed that the geometry, tissue density, and total blood volume remain constant for each tumor type and condition (Tables S1, S2). The optimized model (Supporting Information, Table S2) shows good agreement with the complete set of experimental data (Table 4), with iRGD causing a 4.5-fold increase in P (Table S3).

To validate this model we used an independent set of data, i.e., the availability of receptors to the biotinylation probe. The sulfo-NHS-LC-biotin used in this study is considered to be membrane impermeable, passing through pores in or between cells to reach tissue targets beyond the endothelial layer. This reagent is frequently used for the identification and quantification of proteins on cell membranes, although proteins annotated to subcellular localizations may also be labeled[12]. In our study, the data from M21 tumors show that 14% of the accessible receptors without using iRGD belong to host mouse endothelial cells while the rest are from tumor cells (Table S4). This indicates that the biotinylation reagent is indeed able to cross the endothelial layer. The large excess of biotinylation compound (~2 mM) in the perfusion solution over vascular receptors promotes the diffusion and reaction in the perivascular tissue[8], and mimics certain aspects of a high concentration of targeting probe binding to a receptor. Using the rest of the parameters from the antibody simulations we estimated P for the sulfo-NHS-LC-biotin from the biotinylation experimental data. The percentage of labeled antigen predicted by the fitted model is in good agreement with the experimental data for the three tumor types (Table 4). The fitted P and R_{Krogh} values are summarized in Table S3. P for biotinylation (P = 7.9e-9 m/s) is much greater than for the antibody transport, indicating faster movement of lower molecular weight biotin. However, it is slower than reported for other small molecules[13,14], a deviation attributed to the negative charge and limited membrane permeability characteristics of sulfo-NHS-LC-biotin, and consumption of the probe by amines richly present in the interstitial space.

Simulation results. Using the model we plotted the antibody accumulation profile in a tissue cross-section (Figure 4), illustrating how the antibody penetrates deeper into the tumor when iRGD is present. In Figure 4B,C, we compare the effect of the dose of antibody on the

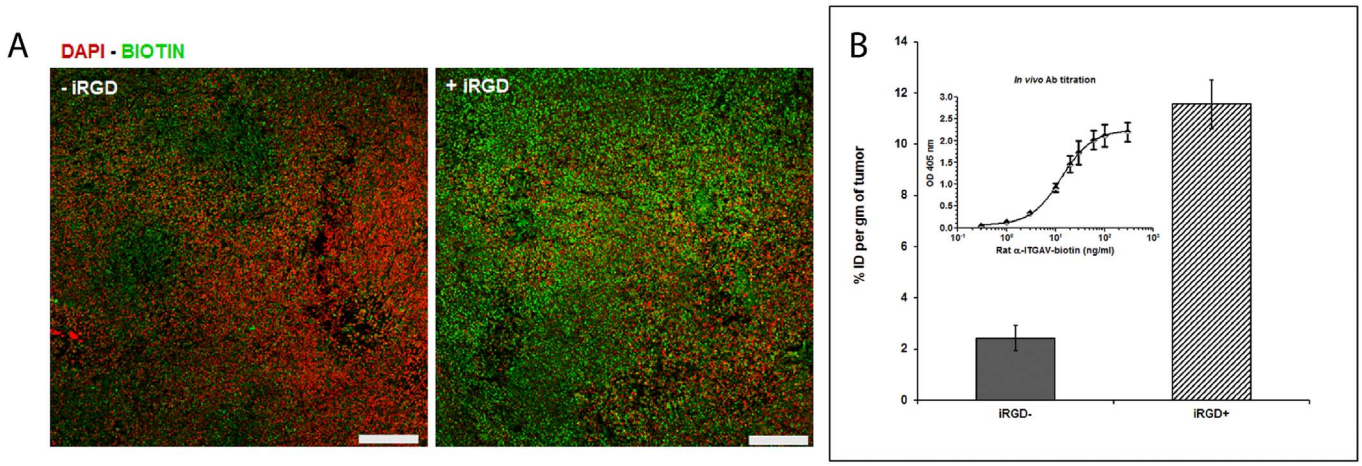

Figure 2 | **Effect of iRGD on antibody accumulation in tumor tissue.** (A) Fluorescence microscopy images of biotin-labeled rat anti-mouse αv with and without prior injection of the tumor penetrating peptide, iRGD. Images representative of at least five sections from each tumor (n = 3 mice per group) are shown. Scale bars = 100 μm. (B) Percentage of injected dose of the antibody per gram tumor (%ID/g) measured by sandwich ELISA. The inset shows the ELISA standard curve.

Table 3 | Experimental and model predicted percentage of injected dose per gram tumor tissue (% ID/g) using the fitted parameters

Tumor	Antibody Dose (μg)	Predicted (%ID/g)	Experiment al (%ID/g)	Predicted (pmol/g)	Experimental (pmol/g)	Experimental (% receptors)
4T1	100 (−iRGD)	**2.64**	2.50	**17.6**	16.6	10.3
	100 (+iRGD)	**11.2**	11.6	**74.4**	77.4	43.3
	60 (−iRGD)	**2.64**	3.07	**10.6**	12.3	6.22
	60 (+iRGD)	**11.2**	10.4	**44.8**	41.8	26.4
BT474	100 (−iRGD)	**4.15**	3.94	**28.6**	27.1	1.53
	100 (+iRGD)	**18.4**	18.4	**126**	128	6.75

The amount of antibody in the tumor tissue after an injection of anti-mouse αv (4T1 tumor mice) or Trastuzumab (BT474 tumor mice) at different concentrations was determined experimentally after 1 h circulation as described the ''Materials & Methods'' section. The effect of iRGD on antibody uptake was evaluated. Data represent the mean %ID/g tissue (n = 3–5 mice per group).

%ID/g, plotting simulation results for 4T1 and BT474 tumors. In the case of 4T1 tumors, the %ID/g decreases slightly for doses above 100 μg when iRGD is present, meaning that saturation of the target is occurring (Ab > Ag, Figure 4B). When iRGD is not included, the initial stage of saturation occurs well above 1000 μg indicative of limited accessibility. For BT474 tumors the saturation with iRGD administration occurs at higher dosage than for 4T1 since BT474 has a greater amount of receptors per tumor volume (Figure 4C). In this tumor model, iRGD increases the %ID/g by 4 to 5 fold across the entire therapeutically relevant dosage window.

Discussion

Information on the quantity and accessibility of targeting receptors in intact tissues is an increasingly important factor to consider in developing targeted therapies. Here we develop methods for both quantifying accessible receptor in tissues and for computational modeling of the kinetics of drug permeation.

The αv integrin and HER2 amount in tumors was as expected; the 40,000 receptors per cell number we measured for αv integrins is typical of cell surface proteins, including integrins[15,16], and the amplification of the HER2 gene in the BT474 cells agreed with the 10 fold higher expression of this protein[17]. Nonetheless, the amount of total receptor available for tumor targeting of drugs is quite limited, only 200–2,000 picomoles per gram of tumor.

An even more sobering number is the relatively small fraction of the receptors that our results show to be available for blood-borne probes, around 5%. Taken together with the total number of receptors in a tumor, it means that only a few picomoles of a drug conjugate can be specifically targeted to a tumor using tumor-specific targeting probes. This figure is likely modified over time by factors such as diffusion of the drug conjugate into the tumor, receptor turnover, modification of entry into cells and other factors, some of which have been modeled in our simulation studies. These factors are likely to have a greater effect when the probe has a long half-life in circulation, such as an antibody.

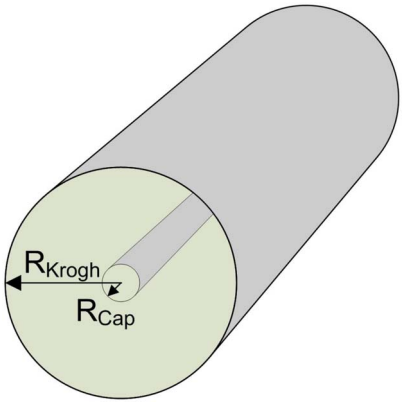

Figure 3 | The geometry of the vascular-tissue model, the Krogh cylinder. A hollow inner cylinder with radius R_{cap} represents a capillary that carries the blood plasma and probe molecules while a semi-permeable endothelial barrier restricts passage between the plasma and the surrounding tissue. Each section of capillary vessel is responsible for supplying blood and the small molecule biotinylation probe, or antibody, to the surrounding cylindrical section of tissue with radius R_{Krogh}.

We found greater availability for the αvβ3 integrin than HER2, despite the 10-fold higher expression of HER2. The likely reason is that the integrin is also expressed in tumor vessels, where all cell surface receptor should be available, whereas HER2 binding requires access to tumor cells. This comparison emphasizes the utility of vascular tumor markers in drug targeting. The differences in the accessibility of the same receptor in different tumors, which we also observed, is likely to be caused by differences in the density of the tumors, which is known to affect drug penetration[18,19]. In addition, the amount of intracellular receptor, which constitutes a substantial fraction of the total receptor[20,21], may vary from tumor to tumor.

Higher receptor saturation densities than ours have been observed, particularly with antibodies[22,23]. However, these authors used the test antibodies in large excess relative to the receptor, which is not advisable in synaphic targeting because exceeding the capacity of the receptors will defeat the purpose of the targeting. We also used the biotinylation probe in excess to detect available receptor. Thus, it should be noted that the biotinylation analysis probably overestimates the number of receptors readily available for synaphic targeting, particularly in the relatively short time frame we used.

A recently identified tumor-penetrating peptide, iRGD, promotes the entry of coupled and co-injected compounds into tumor tissue through a transport pathway specifically activated in tumors[2,3]. Our modeling results identify vascular permeability as the modeling parameter most relevant to iRGD-enhanced treatment. Permeability is used here as an operational term that describes the transport across the endothelial layer separating the blood volume from the tissue. It does not include details involving the biological mode of the transport, e.g. endocytosis, transcytosis, or convection flow.

One finding of this study is that the increase in tumor accumulation for the targeted drugs by iRGD was effective for both biotin and antibody penetration. Earlier studies have shown that tumor accumulation of compounds ranging from simple drugs to nanoparticles is enhanced by iRGD co-administration[3]. Thus, the iRGD effect is general, and minimally dependent on the size and hydrophilicity of the drug. Here, we examined the effects of a single injection of iRGD in the one-hour window that has been observed for iRGD[3]. The pharmacokinetic model we have developed can be used to model drug transport, and this model suggests that iRGD enhances the effective vascular permeability, which increases receptor accessibility and drug accumulation in the tumor. This effect is likely to be particularly pronounced for compounds with a short half-life in the circulation because they have a limited time window to penetrate into extravascular tumor tissue.

Even with the aid of approaches such as using iRGD, these numbers still mean that only picomoles of a drug can be specifically delivered per gram of tumor using targeting probes. Few drugs have specific activities compatible with these numbers, which emphasizes

Table 4 | Predicted vs experimental percentage (%) of labeled antigen for the three tumor types considered in this study (4T1, M21, and BT474)

Tumor	iRGD	Predicted % labeled Ag	Experimental % labeled Ag
4T1	–	4.2	4.3
	+	18.7	20
M21	–	9.0	9
	+	39.8	38
BT474	–	7.7	5.7
	+	33.8	33.1

the importance of selecting drugs that have the highest possible specific activities for synaphic targeting. These quantitative aspects of targeting have generally been underappreciated, and exceeding the receptor capacity is likely to be the most common reason for failures in attempt to deliver drugs using the targeting approach. Using multiple receptors at the same time would be one solution, but it would not change the fact that most of the available receptors will not be available for the drug conjugate to bind to. Our experimental data provide a quantitative basis for assessing the magnitude of the problem and the mathematical model we have developed allows the assessment of the parameters that are most likely to help deal with it.

Methods

Antibodies and reagents. The anti-integrin αvβ3 monoclonal antibody LM609 was purchased from Millipore (Hayward, CA). The goat anti-human integrin αv polyclonal antibody was obtained from R&D systems (Minneapolis, MN), and the biotin-labeled, rat anti-mouse integrin αv monoclonal antibody was from eBioscience (San Diego, CA). The anti-biotin BN34 mouse monoclonal antibody was from Sigma Life Sciences (St. Louis, MO), and trastuzumab (Herceptin) was kindly provided by Dr. Daniel Greenwald of the Cancer Center of Santa Barbara. Horseradish peroxidase (HRP) conjugated goat anti-rat and donkey anti-goat secondary antibodies were from Millipore and R&D systems, respectively. Recombinant human integrin αvβ3 and HER2-Fc chimeras were purchased from R&D systems. Sulfo-NHS-LC-biotin and biotin quantitation kit were from Pierce (Rockford, IL). The 2,2-azino-bis(3-ethylbenzothiazoline-6-sulfonic acid) and all other reagents of analytical and molecular biology grade were obtained from Sigma-Aldrich. iRGD peptide with sequence Ac-{CRGDKGPDC}-NH_2 was synthesized in house as described[2].

In vivo tumor models. The M21 human melanoma cancer cell line was cultured in Dulbecco's Modified Eagle Medium (DMEM) with 10% fetal bovine serum (FCS) and penicillin/streptomycin. The BT474 human breast cancer cell line was cultured in DMEM/F12 (1 : 1) medium with 10% FCS and penicillin/streptomycin. The mouse 4T1 breast cancer cells were cultured in Ischove's Modified Dulbecco Medium (IMDM; Invitrogen) supplemented with 10% FCS and penicillin/streptomycin. For the 4T1 xenografts, 1×10^6 cells were injected orthotopically into BALB/c mice (Charles River, Wilmington, MA). The M21 model was generated by injecting 1×10^6 cells subcutaneously (s.c.) into the flanks of female nude mice (Harlan Sprague Dawley, Inc., Indianapolis, IN). For the BT474 xenografts, 17β-estradiol pellets (Innovative Research of America, Sarasota, FL) were implanted s.c. into the back of the nude mice one day prior to the orthotopic inoculation of 5×10^6 cells in matrigel (BD Biosciences, San Jose, CA). We avoided using tumours that had grown big enough to have necrosis. All animal experimentation was performed according to procedures approved by the Animal Research Committee at the University of California, Santa Barbara.

In vivo biotinylation. To specifically quantify accessible αvβ3 integrin and HER2 receptors we labeled proteins accessible from the blood circulation with perfusion of amine-reactive biotin[8,24] and quantified labeled target and total target protein by ELISA. Anesthetized tumor mice were terminally perfused, first with a solution of 10% dextran-40 (w/v) in PBS at 37°C to remove blood and then with 1 mg/mL sulfo-NHS-LC-biotin in PBS containing 10% Dextran-40 (w/v), followed by neutralization of the unreacted biotinylation reagent with 50 mM Tris(hydroxymethyl) aminomethane hydrochloride in PBS (Tris, pH 7.4). Tissues and tumors were excised, and either snap-frozen to prepare homogenates or embedded in Tissue-Tek O.C.T (Fisher Scientific, USA) for cryopreservation and sectioning.

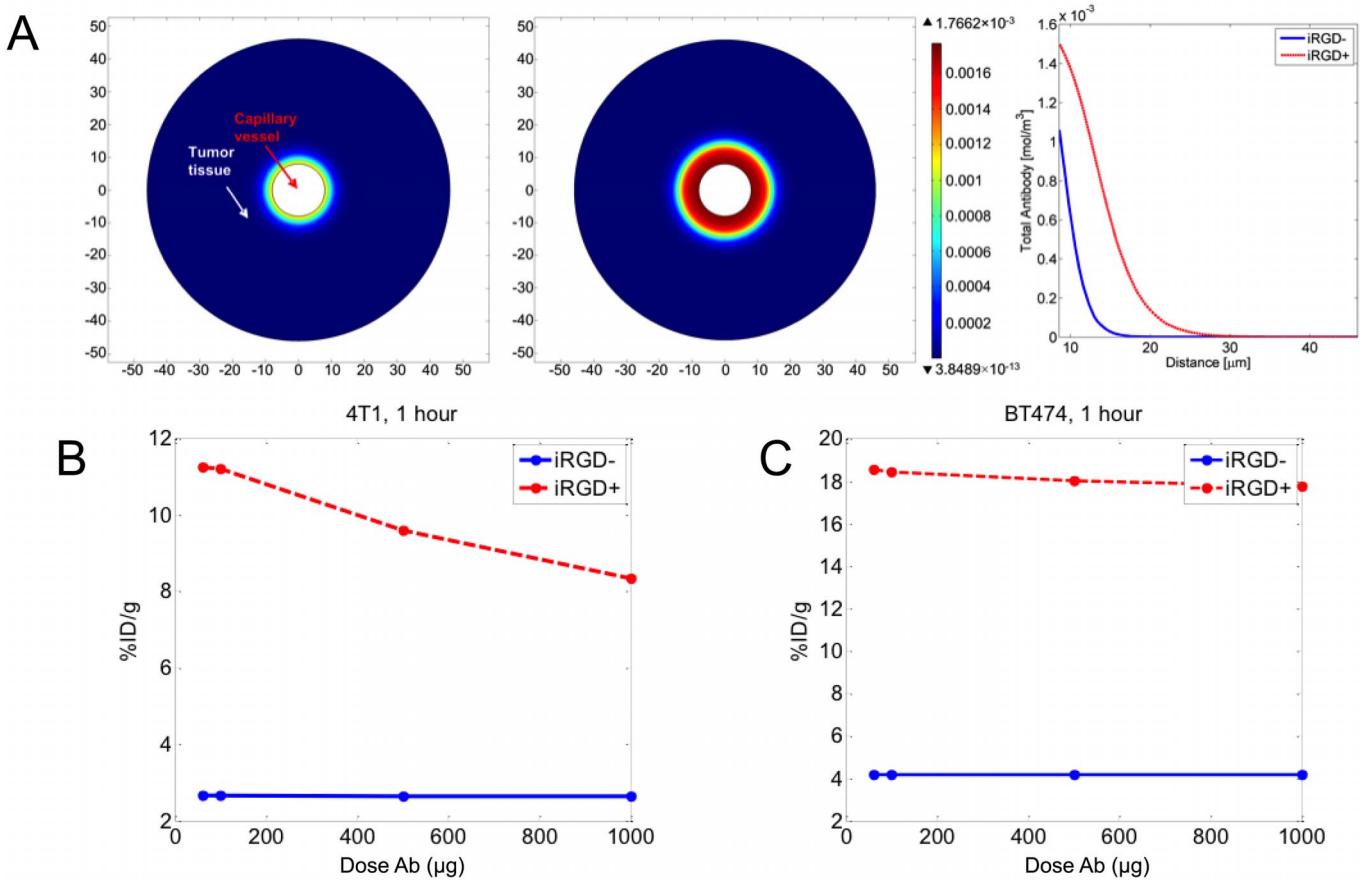

Figure 4 | (A) Tumor total antibody concentration profile after 1 h circulation for BT474 illustrating how the antibody penetrates deeper into the tumor when iRGD is present. (B) Plot of simulation %ID/g vs Antibody (Ab) dose after 1 h circulation with and without iRGD for the 4T1 tumor model and (C) for BT474 tumor model.

Immunofluorescence analysis of biotinylated tissues and tumour. Cryosections (6 μm thickness) were incubated with Streptavidin-Alexa Fluor 488 (Molecular Probes) to visualize labelling. The nuclei were stained with DAPI. Tissue sections were examined and photographed under a FluoView 500 confocal laser-scanning microscope (Olympus).

Preparation of protein extracts and receptor quantification. Tumours from *in vivo* biotinylated mice were suspended in lysis buffer (2% NP-40, 50 mM Tris, 10 mM EDTA, protease inhibitor cocktail) in PBS at 50 mg tumor per mL lysis buffer. The samples were homogenized, sonicated for 5 min and centrifuged at 16000 × g for 10 min at room temperature. Protein concentration in the supernatant was quantified by the BCA assay (Pierce). To determine the number of biotinylated αvβ3 receptors, ELISA plates were coated with 50 μl of goat anti-human αv polyclonal antibody at a concentration of 5 μg/mL for 18 h at 4°C. The wells were washed three times with PBS/0.05% Tween-20, and blocked with 1% biotin-free BSA. Diluted tumor lysates or biotinylated standards of αvβ3 and HER2 (*described in the following section*) were added to the wells and incubated for 2 hr at room temperature with shaking. After washing, 100 μL of streptavidin-HRP (diluted 1 : 1000) in 1% BSA/PBST (PBS with 0.05% Tween 20) was added to the wells and incubated with shaking for 30 min at RT. The plates were then developed with 2,2-azino-bis(3-etylbenzthiazoline-6-sulfonic acid) and absorbance measured at 405 nm. To separately quantify human and mouse αvβ3 integrins in M21 xenograft tumor lysates, sandwich ELISA was performed with species-specific anti-human αvβ3 LM609 and rat anti-mouse αv monoclonal antibodies. The biotinylation of HER2 receptor in the BT474 model was similarly quantified by direct sandwich ELISA using anti-human HER2 (Herceptin) as the capture antibody.

Total number of αvβ3 or HER2 receptors in tumour extracts was quantified by competition ELISA (refer to Figure S1C). ELISA plates were coated with the respective capture antibodies, goat anti-integrin αv polyclonal antibody (4T1), anti-human integrin αvβ3 monoclonal antibody LM609 (M21), or Herceptin (BT474). Serially diluted standards (αvβ3 or HER2), or tumour extracts, were pre-mixed with biotinylated recombinant αvβ3 or HER2 in 1% BSA/PBST, and added to their respective wells. After incubation for 1 h at 37°C, wells were washed and streptavidin-HRP was added to the wells. Following incubation and washing, the plates were developed with 2,2-azino-bis(3-ethylbenzothiazoline-6-sulfonic acid) and absorbance measured at 405 nm.

Biotinylation of recombinant *αvβ3* and *HER2* proteins. For quantifying accessible receptors for antibody injection experiments, recombinant αvβ3 integrin and HER2-Fc extracellular domain (ECD) were biotinylated using the micro sulfo-NHS-biotinylation kit (Pierce) according to the manufacturer's protocol, and the biotinylated protein was purified with a desalting column. The degree of biotinylation was determined using the 2-(4-Hydroxyphenylazo)benzoic acid (HABA) assay (Pierce). The proteins biotinylated by this procedure carried on average 2.4 - 3.1 biotin molecules per molecule of protein.

Injection of biotinylated antibodies. To study the effect of the tumor-penetrating peptide iRGD[3] on receptor availability towards antibodies, 100 μL of 200 μM iRGD or PBS were intravenously injected into mice bearing 4T1 or BT474 tumors. Thirty minutes later, biotinylated rat anti-mouse αv (for 4T1 tumor mice) or trastuzumab (for BT474 tumor mice) was injected at different concentrations. After 1 h circulation the mice were perfused with PBS, tumors excised and either snap-frozen or embedded in O.C.T for cryopreservation and sectioning.

In silico modeling. A computational model based on partial differential equations (PDEs) was developed to describe the diffusion of probes through the blood vessels and the non-vascular tumor tissue. The model builds on the work of Thurber et al.[25] which is relevant for antibody uptake and retention in vascularized tumors. The foundation of the model includes the major processes affecting the time course of antibody concentration delivered to a tumor (see Supporting Information). The complete set of processes includes local and systemic clearance, extravasation, diffusion, binding, release, endocytosis, recycling, and degradation and can be applied to the geometry of interest. As a simple vascular-tissue model we chose a two-dimensional representation using the Krogh-like cylinder geometry; a blood vessel is visualized by extending the concentric circles in the third dimension (Figure 3). A hollow inner cylinder carries the blood plasma and probe molecules while a semi-permeable endothelial barrier restricts passage between the plasma and the surrounding tissue. Each section of capillary vessel is responsible for supplying blood and the small molecule biotinylation probe, or antibody, to the surrounding cylindrical section of tissue (Figure 3). The vasculature is represented as an array of concentric capillaries in tissue in close-packed configuration; the outer surface of tissue cylinders defines the region where outward transport balances the inward transport from proximal cylinders. See Supporting Information for more detail.

1. Ruoslahti, E., Bhatia, S. N. & Sailor, M. J. Targeting of drugs and nanoparticles to tumors. *J Cell Biol* **188**, 759–768 (2010).
2. Sugahara, K. N. *et al.* Tissue-penetrating delivery of compounds and nanoparticles into tumors. *Cancer Cell* **16**, 510–520 (2009).
3. Sugahara, K. N. *et al.* Coadministration of a tumor-penetrating peptide enhances the efficacy of cancer drugs. *Science* **328**, 1031–1035 (2010).
4. Desgrosellier, J. S. & Cheresh, D. A. Integrins in cancer: biological implications and therapeutic opportunities. *Nat Rev Cancer* **10**, 9–22 (2010).
5. Ruoslahti, E. Peptides as targeting elements and tissue penetration devices for nanoparticles. *Adv Mater* **24**, 3747–3756 (2012).
6. Al-Dasooqi, N., Gibson, R., Bowen, J. & Keefe, D. HER2 targeted therapies for cancer and the gastrointestinal tract. *Curr Drug Targets* **10**, 537–542 (2009).
7. Arteaga, C. L. *et al.* Treatment of HER2-positive breast cancer: current status and future perspectives. *Nat Rev Clin Oncol* **9**, 16–32 (2012).
8. Rybak, J. N. *et al.* In vivo protein biotinylation for identification of organ-specific antigens accessible from the vasculature. *Nat Methods* **2**, 291–298 (2005).
9. Fleming, J. M., Miller, T. C., Meyer, M. J., Ginsburg, E. & Vonderhaar, B. K. Local regulation of human breast xenograft models. *J Cell Physiol* **224**, 795–806 (2010).
10. DeVita, V. T., Jr., Young, R. C. & Canellos, G. P. Combination versus single agent chemotherapy: a review of the basis for selection of drug treatment of cancer. *Cancer* **35**, 98–110 (1975).
11. Del Monte, U. Does the cell number 10(9) still really fit one gram of tumor tissue? *Cell Cycle* **8**, 505–506 (2009).
12. Strassberger, V., Trussel, S., Fugmann, T., Neri, D. & Roesli, C. A novel reactive ester derivative of biotin with reduced membrane permeability for in vivo biotinylation experiments. *Proteomics* **10**, 3544–3548 (2010).
13. Dreher, M. R. *et al.* Tumor vascular permeability, accumulation, and penetration of macromolecular drug carriers. *J Natl Cancer Inst* **98**, 335–344 (2006).
14. Wu, N. Z., Klitzman, B., Rosner, G., Needham, D. & Dewhirst, M. W. Measurement of material extravasation in microvascular networks using fluorescence video-microscopy. *Microvasc Res* **46**, 231–253 (1993).
15. Benedetto, S. *et al.* Quantification of the expression level of integrin receptor alpha(v)beta3 in cell lines and MR imaging with antibody-coated iron oxide particles. *Magn Reson Med* **56**, 711–716 (2006).
16. Beer, A. J. *et al.* Positron emission tomography using [18F]Galacto-RGD identifies the level of integrin alpha(v)beta3 expression in man. *Clin Cancer Res* **12**, 3942–3949 (2006).
17. Shi, Y. *et al.* A novel proximity assay for the detection of proteins and protein complexes: quantitation of HER1 and HER2 total protein expression and homodimerization in formalin-fixed, paraffin-embedded cell lines and breast cancer tissue. *Diagn Mol Pathol* **18**, 11–21 (2009).
18. Grantab, R., Sivananthan, S. & Tannock, I. F. The penetration of anticancer drugs through tumor tissue as a function of cellular adhesion and packing density of tumor cells. *Cancer Res* **66**, 1033–1039 (2006).
19. Rejniak, K. A. *et al.* The role of tumor tissue architecture in treatment penetration and efficacy: an integrative study. *Front Oncol* **3**, 111 (2013).
20. Wiley, H. S. & Cunningham, D. D. The endocytotic rate constant. A cellular parameter for quantitating receptor-mediated endocytosis. *J Biol Chem* **257**, 4222–4229 (1982).
21. Ghaghada, K. B., Saul, J., Natarajan, J. V., Bellamkonda, R. V. & Annapragada, A. V. Folate targeting of drug carriers: a mathematical model. *J Control Release* **104**, 113–128 (2005).
22. Berk, D. A., Yuan, F., Leunig, M. & Jain, R. K. Direct in vivo measurement of targeted binding in a human tumor xenograft. *Proc Natl Acad Sci U S A* **94**, 1785–1790 (1997).
23. Rhoden, J. J. & Wittrup, K. D. Dose dependence of intratumoral perivascular distribution of monoclonal antibodies. *J Pharm Sci* **101**, 860–867 (2012).
24. Roesli, C., Neri, D. & Rybak, J. N. In vivo protein biotinylation and sample preparation for the proteomic identification of organ- and disease-specific antigens accessible from the vasculature. *Nat Protoc* **1**, 192–199 (2006).
25. Thurber, G. M., Zajic, S. C. & Wittrup, K. D. Theoretic criteria for antibody penetration into solid tumors and micrometastases. *J Nucl Med* **48**, 995–999 (2007).

Acknowledgments

We thank Kazuki N. Sugahara and Tambet Teesalu for helpful discussions. This work was supported by grant CA152327 and Cancer Center Support grant CA30199 from the NCI, and by the Institute for Collaborative Biotechnologies through grant W911NF-09-0001 from the U.S. Army Research Office. The content of the information does not necessarily reflect the position or the policy of the Government, and no official endorsement should be inferred. G.B.B. was supported by fellowships from the Cancer Center of Santa Barbara and the NIH (T32 CA121949).

Author contributions

S.H., M.R.F., G.B.B., F.D.III. and E.R. designed the experiments and analyzed the results; S.H. carried out the experiments; M.R.F. performed the simulation analyses; S.H., M.R.F., G.B.B., F.D.III. and E.R. wrote the manuscript.

Additional information

Supplementary information accompanies this paper at http://www.nature.com/scientificreports

Competing financial interests: E.R. has ownership interest (including patents) in CendR Therapeutics Inc. E.R. is the founder, chairman of the board, consultant/advisory board member, and major shareholder of CendR Therapeutics Inc., and has ownership interest

(including patents) in the same. E.R. is also a consultant/advisory board member, and major shareholder of EnduRx Pharmaceuticals Inc., and has ownership interest (including patents) in the same. No potential conflicts of interest were disclosed by the other authors.

How to cite this article: Hussain, S., Rodriguez-Fernandez, M., Braun, G.B., Doyle, F.J. & Ruoslahti, E. Quantity and accessibility for specific targeting of receptors in tumours. *Sci. Rep.* **4**, 5232; DOI:10.1038/srep05232 (2014).